Influence of Sm-Mn Substitution on Structural, Dielectric and Electrical Properties of X-Type Hexagonal Nanoferrites

[1]Imran Sadiq, [1]Imran Khan, [2]Evgeny V. Rebrov, [3]M. Naeem Ashiq*, [4]Shahzad Naseem, [5]Imran Shakir and [1]Mazhar. U.Rana**

[1]*Department of Physics, Bahauddin Zakariya University, Multan 60800, Pakistan.*
[2]*School of Chemistry and Chemical Engineering, Queen's University Belfast, UK.*
[3]*Institute of Chemical sciences, Bahauddin Zakariya University, Multan 60800, Pakistan.*
[4]*Centre for Solid State Physics, University of Punjab, Lahore, Pakistan.*
[5]*Sustainable Energy Technologies (SET) center, College of Engineering, King Saud University, Kingdom of Saudi Arabia*
naeemashiqqau@yahoo.com*, mazharrana@bzu.edu.pk**

(Received on 20th February 2013, accepted in revised form 14th October 2013)

Summary: A series of Sm-Mn substituted X-type hexagonal ferrites with composition $Sr_{2-x}Sm_xNi_2Fe_{28-y}Mn_yO_{46}$ (x=0.02, 0.04, 0.06, 0.08, .010 and y= 0.1, 0.2, 0.3, 0.4, 0.5) have been synthesized by sol gel method. The temperature at which required phase has been obtained was confirmed from the TGA/DSC analysis. X-Rays Diffraction analysis reveals the single phase of the prepared material. The lattice parameters and unit cell volume change with substitution of Sm-Mn contents. SEM and TEM analysis indicates that the crystallite size lies in the range of 60-80 nm. The dielectric constant decreases with the increase of frequency. The relaxation peaks in tangent loss curves indicates the presences of polarons in the material and make this material applicable in medium frequency (MF) devices. The results of electrical resistivity measurements indicate the enhancement in room temperature resistivity with the substitution of Sm-Mn contents. The increase in resistivity reflects the applications of synthesized material in microwave devices and reducing the eddy current losses.

Keywords: Hexagonal Ferrites; structural properties; TEM; Electrical properties; Dielectric properties.

Introduction

The usage of high frequency electronics devices in our daily life has been abruptly increased during the recent years so the electromagnetic wave interference (EMI) and electromagnetic radiation pollution have become a serious problem. Devices malfunction, formation of false images and inconsistent radar signals are the known effects of EMI. That is why wireless devices such as hand phones, computers and pagers are banned from being used at some specific places and times in hospitals, banks and aero planes [1-4]. In Medical, some devices can easily be disturbed by EMI such as; magnetic resonance, microwave and ultrasound imaging. It is also noticed that hearing aids, servo-ventilator and surgical electrical appliances are the medical devices that should be needed to protect from EMI. The above mentioned studies clearly indicate the importance of the works designed in minimizing exposure to microwave on biological as well as electronic systems by using advancement in absorber technology [5]. Hexaferrites are the suitable materials for microwave absorption due to their high magnetization, high resistivity, good dielectric properties and excellent chemical stability [6]. Among the hexagonal ferrites, X-type hexagonal ferrites with chemical formula $Ba(Sr)_2M_2Fe_{28}O_{46}$ (M: Fe^{2+},Co^{2+},Zn^{2+},Mg^{2+}, etc.) can be considered good for absorption properties [7]. It has been reported that the magnetic and dielectric properties of ferrites can be controlled by rare earth substitution [8].

Many researchers reported the dielectric properties of rare earth substituted hexagonal ferrites. J.Xu *et al* [9] prepared the Sm^{3+}substituted hexagonal ferrites by using conventional ceramic sintering method. The samples were characterized by XRD, FESEM, VSM and network Analyzer. The decrease in grain size and enhancement in magnetic properties with the substitution of Sm^{3+} was observed. The sample with concentration x=0.10 shows maximum value of complex (ε', ε") permittivity. The value of imaginary part (μ") of complex permeability decreases after Sm^{3+} substitution while no change observed in real part (μ') of complex permeability with Sm^{3+} substitution for all samples which has been discussed using electromagnetic theory. However, the dielectric properties of rare earth Sm^{3+} substituted X-type hexagonal nanoferrites have seldom been reported, that is why we choose this material for our investigation.

The aim of present work is to control the magnetic and electrical properties by substituting rare earth element $Sm^{3+}$and to make materials suitable in electronics devices. The effect of rare earth

*To whom all correspondence should be addressed.

substitution on structural, electrical and dielectric properties has also discussed.

Experimental

The X-type hexagonal ferrites samples with composition Sr_{2-x} $Sm_xNi_2Fe_{28-y}Mn_yO_{46}$ (x=0.02, 0.04, 0.06, 0.08, .010 and y= 0.1, 0.2, 0.3, 0.4, 0.5) were prepared by the sol-gel method. The stoichiometric ratio of raw materials ($Sr(No_3+_2$, $Mn(No_3)_2$, $NiCl_2$. $6H_2O$, Sm_2O_3, Iron nitrate, Citric Acid) were mixed in deionized water. The gel was obtained by evaporating the solution at 80˚C. The gel was burnt at 400˚C f or 1 hour and finally sintered at 1250˚C for 6 hours to attain the required phase. The powder was then pressed into pellets at a pressure of (~30KN) using Paul-Otto Weber hydraulic press by using Polyvinyl alcohol as a binder. The thermal analysis to conform the temperature at which required phase can be obtained was carried out by the Mettler Toledo TGA/DSC 1 STAR^e system equipped with Nitrogen gas. The crystalline phase after heat treatment was identified by Schimadzu X-ray diffractometer which uses Cu-K_a as a radiations source (λ =1.5406Å). The surface morphology and particle size was examined by JEOL JSM- 6500F field emission scanning electron microscopy (FESEM) and TECNAI F20 Phillips High Resolution Transmission Electron Microscopy (HRTEM). The electrical properties were measured by the two probe method, using sensitive source meter model Keithly 2400.The frequency dependent dielectric properties were measured by using LCR meter.

Results and discussion

Figure 1 shows the TGA curve from room temperature to 1000 ˚C for the pre-calcined precursor at 400˚C for 1 hour. A wide endothermic curve with weight loss of 3.32% from room temperature to 440 ˚C can be observed in TGA curve. This can be attributed to the removal of free and hydrated water. However another wide endothermic peak starts from 450˚ C with weight loss of 3.31% indicates the removal and oxidation of organic compounds. The wide exothermic peak in the end of the curve may show the formation of hexagonal structure. Fig1 b shows the DSC curve from room temperature to 500 ˚C for the pre-calcined material at 400˚C for 1 hour. The two endothermic peaks at 55˚C and 141 ˚C may show the dehydration of water absorbed by the pre-calcined precursor and the exothermic peak at 450 ˚C which shows the weight loss in TGA can be attributed to the removal of organic compounds and substituent's. The TGA and DSC data is in good agreement with each other.

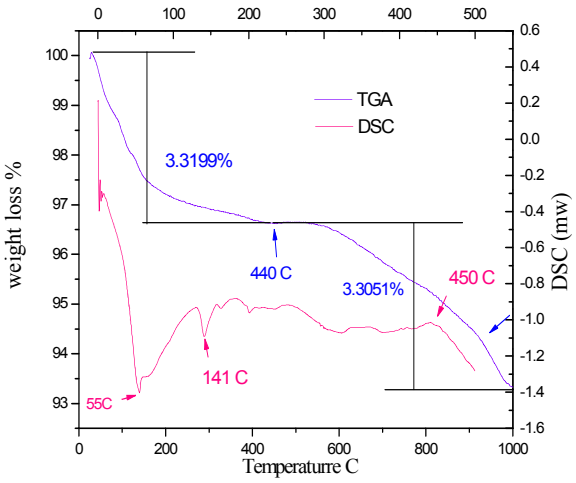

Fig. 1: TGA and DSC analysis of precursor pre-sintered at 400 ˚C.

The X-ray diffraction patterns for Sr_{2-x} $Sm_xNi_2Fe_{28-y}Mn_yO_{46}$ (x=0.02, 0.04, 0.06, 0.08, .010 and y= 0.1, 0.2, 0.3, 0.4, 0.5)hexagonal ferrites prepared by sol-gel method are shown in Fig. 2.All the diffraction peaks matched with JCPDS # 790496 which indicates the single phase of all the samples. However two peaks at 2θ values 40.12 and 69.53 have been disappeared with the substitution of Sm-Mn contents. The lattice parameters a (Å) and c(Å) were calculated by using the following Equation

$$1/d^2_{hkl} = 4\,(h^2+hk+k^2) / 3a^2 + l^2/c^2 \qquad (1)$$

where d_{hkl} is the d-spacing of the lines in the XRD pattern and h, k and l are the corresponding Miller indices.

Table-1: Lattice parameters, cell volume, and resistivity of Sr_{2-x} Sm_x Ni_2 $Fe_{28-y}Mn_yO_{46}$ (x=0.00, 0.02, 0.04, 0.06, 0.08, .010 and y= 0, 0.1, 0.2, 0.3, 0.4, 0.5) at 1250˚C for 6 hours

Parameters	x= 0	x=0.02	x= 0.04	x=0.06	x=0.08	x=0.10
Lattice constanta (Å)	5.6 967	5.6932	5.6900	5.6872	5.6890	5.6912
Lattice constantc (Å)	81.1967	81.1970	81.1999	81.2014	81.2072	81.2005
Unit cell volume (Å)^3	2282	2279.21	2276.72	2274.54	2276.12	2277.70
Resistivity (Ωcm) x 10^7	1.1	3.3	5.8	6.9	7.3	23

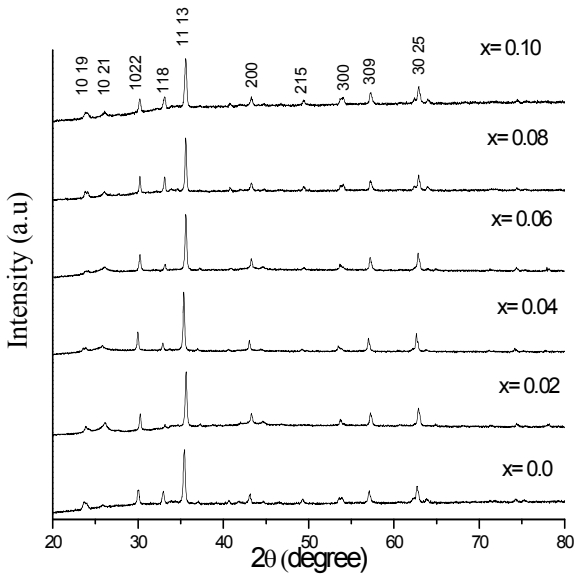

Fig. 2: XRD patterns of Sr_{2-x} Sm_x Ni_2 $Fe_{28-y}Mn_yO_{46}$ (x=0.00,0.02, 0.04, 0.06, 0.08, .010 and y= 0, 0.1, 0.2, 0.3, 0.4, 0.5) at 1250˚C for 6 hours.

The unit cell volume was calculated by using following formula

$$V = a^2 c \sin 120^\circ \qquad (2)$$

where "a" and "c" are lattice constants.

The variation of lattice parameters a (Å), c (Å) and unit cell volume as a function of Sm-Mn contents is shown in Fig. 3. It is clear from the figure that the lattice constant a (Å) decreases while c (Å) increases with the substitution of Sm-Mn contents. This variation can be explained on the basis of distribution of ions in different sites. B.X. Gu *et al* [10] reported that the Fe lies in the tetrahedral and octahedral sites of the S (Spinal) block while the divalent ion Mn also prefers to occupy the octahedral and tetrahedral sites of the S block. So the substitution of Fe^{3+}(0.645Å) by Mn^{2+}(0.46Å) leads to the decrease the distance among the layers and decrease in the plan a (Å)axis. Another remarkable argument for the variation of lattice parameters can be attributed to the substitution of Sr^{2+} (1.12Å) by Sm^{3+}(0.964Å) results the negative microstrain which produce the compressive stress among the layers which leads to the decrease in the lattice parameters and unit cell volume.

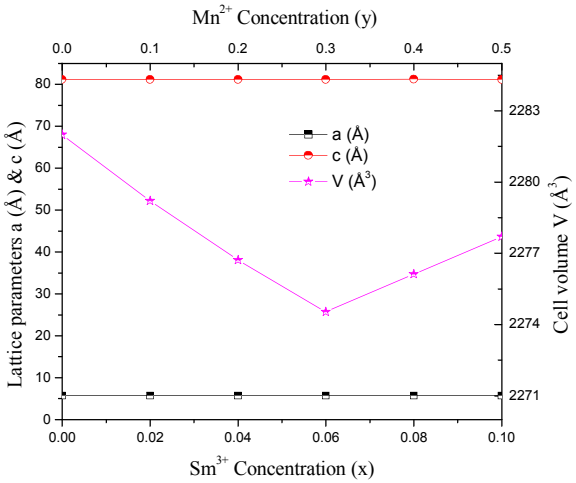

Fig. 3: Variation of lattice constants a (Å), c (Å) and unit cell volume with Sm^{3+} concentration (x) and Mn^{2+} concentration (y).

Fig.4 shows the SEM, HRSEM, TEM and HRTEM micrographs for the present investigated ferrites. It could be observed from the low resolution SEM micrograph that the grains are hexagonal in shape (Fig 4a). The crystallite size is found to be in the range of 60-80 nm and can be seen from the HRSEM micrograph (Fig 4b). The crystallite size measured theoretically from the Scherrer formula lies in the range of 61-75 nm, so the experimentally observed data is in good agreement with the theoretical data. The TEM analysis (Fig 4c) shows that the large number of nanoparticles agglomerate to each other to form the big grain. The regular repeats (Fig 4d) show that the material is well crystallized without any lattice defect and other stacking variants. The planar space of the lattice fringes is about 0.2603 nm which agrees well with the (118) lattice planes of the hexagonal ferrite material.

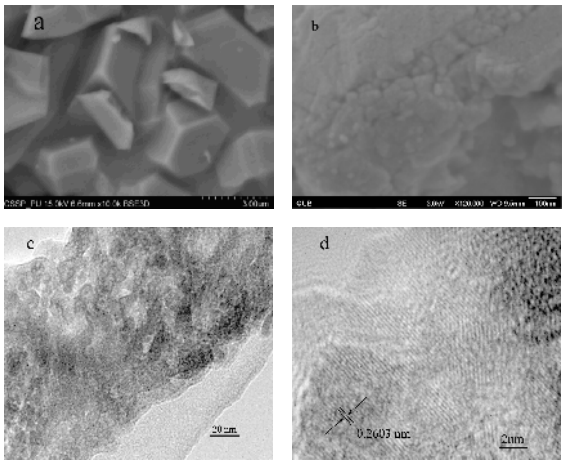

Fig. 4: SEM (a), FESEM (b), TEM (c), HRTEM (d) images for the x-type hexagonal ferrites.

Fig.5 shows the variation of dielectric constant with frequency. The enhancement in the value of dielectric constant can be observed clearly with the increase of Sm-Mn contents. It is worth noting that the dielectric constant decreases with the increase of frequency which is the normal behavior of the hexagonal ferrites. This behavior of dielectric constant with frequency can be explained on the basis of Koop's theory [11] which imagines the dielectric medium as inhomogeneous medium with two Maxwell and Wegner type layers [12,13]. According to this model, the dielectric material is composed of the highly conducting grains separated by the low conducting grains boundaries. Rezlescue model [14] stated that the dielectric polarization mechanism in ferrites is similar to the conduction mechanism. The ferrites conducting grains are effective on high frequency and poorly conducting grains boundaries play a major role on low frequencies and therefore responsible for the high dielectric constant at low frequencies. The high value of dielectric constant at low frequencies can also be attributed to the predominance of the species like Fe^{2+}, interfacial dislocation pile-ups, oxygen vacancies and grain boundary defects [13].

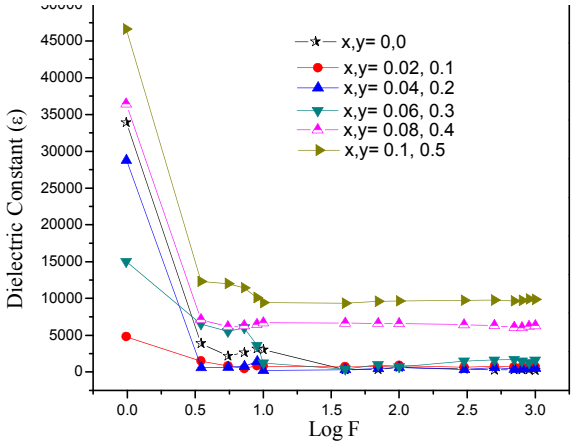

Fig. 5: Variation of the dielectric constant (ε) of (x=0.00, 0.02, 0.04, 0.06, 0.08, .010 and y= 0, 0.1, 0.2, 0.3, 0.4, 0.5) with frequency.

Dielectric tangent loss is important part of the total core loss in ferrite. Low core loss requires low dielectric losses. The value of tangent loss is dependent on various factors such as stoichiometry, Fe^{2+} contents and structural homogeneity and sintering temperature of the samples [15]. The variation of tangent loss with frequency can be observed from the Fig. 6. The abnormal dielectric behavior can easily be observed from the Fig. The conduction mechanism in ferrites is believed to be due to the hopping of electrons between Fe^{2+}/ Fe^{3+} at octahedral sites. As such, when the hopping frequency coincides to the externally applied frequency, resonance occurs, the relaxation peaks come into existence. Another quantitative explanation of the abnormal dielectric behavior can be attributed to the presence of polarons [16]. The presence of small polarons is probable in solid materials with narrow conducting bands and large coupling constant [17]. As the overlap of 3D waves function in neighboring metal ions is small in oxides of the iron group metals especially in ferrites so, the formation of small polarons and hopping process is very probable.

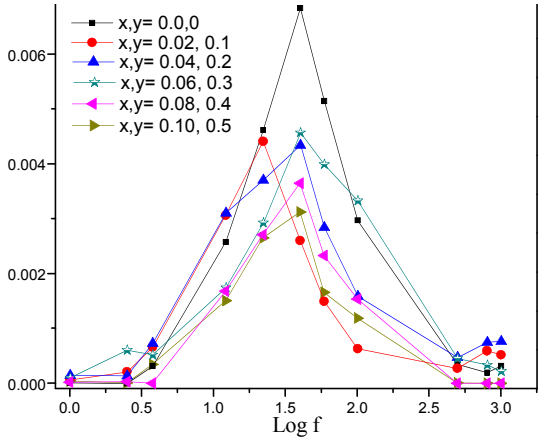

Fig. 6: Variation of the tangent loss (tanδ) of (x=0.00, 0.02, 0.04, 0.06, 0.08, .010 and y= 0, 0.1, 0.2, 0.3, 0.4, 0.5) with frequency.

Fig. 7 shows the variation of room temperature resistivity with Sm-Mn contents in the voltage range of 0-200V. The value of resistivity lies in the range of ~ 10^9 Ωcm. The high value of resistivity shows that the present investigated material could be good candidate to reduce the eddy current losses. It can be seen from the Fig that the Sm-Mn substituted samples have the higher value of resistivity than that of unsubstituted samples. The increase in the resistivity can be explained on the basis of the site occupation of the substituted divalent Mn^{2+} ions. In the case of X-type hexagonal ferrites, the Mn^{2+} ions essentially lie in the octahedral and tetrahedral sites of the spinel S block and most of Fe^{2+}ions lies in the octahedral sites of the spinel S Block [10]. When the substituted divalent Mn^{2+}ions occupy the octahedral sites, then it causes the migration of Fe^{2+} ions towards tetrahedral sites. As a result hopping rate of charge carriers decreases which results the increase in the resistivity of the

synthesized material. It has been reported that Mn^{2+} also converted into Mn^{3+} and created positive holes to maintain the electroneutrality[5]. Now the conduction is due to the transfer of electrons between Fe^{3+} and Fe^{2+}sites as well as due to the transfer of holes between Mn^{2+} and Mn^{3+} sites. The transfer of holes is more difficult as compared to the electrons so as a result the resistivity starts increasing with the substituents. Another quantitative explanation for the increase of the resistivity with the substitution of the Sm-Mn can be attributed to the fact that the dopants Sm(99 x $10^{-6}\Omega$cm) and Mn (139 x $10^{-6}\Omega$cm) are more resistive than the Sr(21.5 x $10^{-6}\Omega$cm) and Fe(9.8 x $10^{-6}\Omega$cm) at room temperature[18].

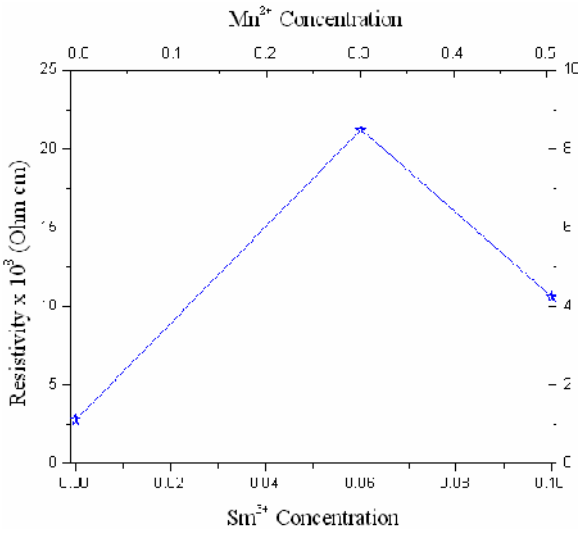

Fig. 7: Variation of resistivity (ρ) with Sm^{3+} (x) and Mn^{2+} (y) concentration.

Conclusions

Sol Gel method is an appropriate method to prepare the X-type hexagonal Nanoferrites. The substitution of rare earth elements results in the changing of the lattice parameters and unit cell volume. SEM micrographs show well hexagonal structures of the grains and the crystallite size lies in the range of 60-80 nm which agrees well with theoretically measured data. The dielectric properties enhances with the substitution of Sm-Mn contents. Room temperature resistivity increases with Sm-Mn contents which reflect its applications in microwave devices.

Acknowledgements

We are thankful to the Higher Education Commission of Pakistan for the financial support in this project. The authors appreciate the support of Dr. Shahzad Naseem, Punjab University Lahore, Pakistan for providing SEM facilities. One of the authors M. N. Ashiq is highly thankful to Higher Education Commission (HEC) of Pakistan for financial support under the project No. 20-1515/R&D/09-8049 and I. Shakir would like extend his sincere appreciation to the Deanship of Scientific Research at King Saud University for its funding to support his research through the Research Group Project no. RGP-VPP-312.

References

1. J. Cao, W. Fu, H. Yang, Q. Yu, Y. Zhang, S. Liu, P. Sun, X. Zhou, Y. Leng, S. Wang, B. Liu and G. Zou, Large-scale synthesis and microwave absorption enhancement of actinomorphic tubular ZnO/$CoFe_2O_4$ nanocomposites, *J. Phys. Chem.* B,**113**, 4642 (2009).
2. Z. Zhang, X. Liu, X. Wang, Y. Wu and R. Li, Effect of Nd–Co substitution on magnetic and microwave absorption properties of $SrFe_{12}O_{19}$ hexaferrites, *J. Alloys Compd.,* **525**, 114 (2012).
3. S. Y. Tong, J. M. Wu, M. J. Tung, W. S. Ko, Y. T. Huang and Y. P. Wang, Effect of Ni concentration on electromagnetic wave absorption of (Ni,Mn,Zn)Fe_2O_4/resin particulate composites, *J. Alloys Compd.,* **525**, 143 (2012).
4. Z. H. Yang, Z. W. Li, L. Liu and L. B. Kong, Enhanced microwave magnetic and attenuation properties of composites with free-standing spinel ferrite thick films as fillers, *J. Magn. Magn. Mater.,* **324**, 3144 (2012).
5. A. N. Yusoff and M. H. Abdullah, Microwave electromagnetic and absorption properties of some LiZn ferrites, *J. Magn. Magn. Mater.,* **269**, 271 (2004).
6. Y. Nie, H. H. He, Z. K. Feng, X. C. Zhang and X. M. Cheng, Microwave characterization of $(Co,Zn)_2W$ barium hexagonal ferrite particles, *J. Magn. Magn. Mater.,* **303**, e423 (2006).
7. Z. Haijun, Y. Xi and Z. Liangying, The preparation and microwave properties of $Ba_2Zn_xCo_{2-x}Fe_{28}O_{46}$ hexaferrites, *J. Magn. Magn. Mater.,* **241**, 441 (2002).
8. GU Ben-xi, LU Huai-xian and DU You-Wei, Magnetic properties and Mössbauer spectra of X type hexagonal ferrites, *J. Magn. Magn. Mater.,* **31**, 803 (1983).
9. J. Xu, G. Ji , H. Zou , Y. Song and S. Gan, Influence of Sm-substitution on structure and electromagnetic properties of

$Ba_{3-x}Sm_xCo_2Fe$
Mater., **323**, 1
10. B. X. Gu, Magnetic properties of *X*-type $Ba_2Me_2Fe_{28}O_{46}$ (Me=Fe, Co, and Mn) hexagonal ferrites, *J. Appl. Phys.,* **71**, 5103 (1992).
11. C. G. Koops, On the dispersion of resistivity and dielectric constant of some semiconductors at audiofrequencies, *Phys. Review*, **83**, 817 (1951).
12. J. C. Maxwell, "A Treatise on Electricity and Magnetism,"Vol. 2 Oxford, New York (1954).
13. K. W. Wagner, Zur theorie der unvollkommenen dielektrika*, Annals der Physik*, **40**, 817 (1913).
14. N. Rezlescue and E. Rezlescu, Cation distribution and Curie temperature in ferrites, *J. Phys. Chem. Solids.,* **23**, 575 (1974).
15. M. J. Iqbal, M. N. Ashiq, P. H. Gomez and J. M. Munoz, Magnetic, physical and electrical properties of Zr–Ni-substituted co-precipitated strontium hexaferrite nanoparticles, *Scripta Materialia*., **57**, 1093 (2007).
16. J. Bao, J. Zhou, Z. Yue, L. Li and Z.Gui, Dielectric behavior of Mn-substituted Co_2Z hexaferrites, *J. Magn. Magn. Mater.*, **250**, 131 (2002).
17. Y. Purushotham and P. V. Reddy, Charge-transport and conduction mechanism of some substituted W type hexagonal ferrites, *Int. J. Mod. Phys. B.*, **10**, 319 (1996).
18. C. Kittle, An introduction to Solid State Physics, 5th edition, John Wiley & sons, New York (1976).